

PERIODICO di MINERALOGIA
established in 1930

*An International Journal of
MINERALOGY, CRYSTALLOGRAPHY, GEOCHEMISTRY,
ORE DEPOSITS, PETROLOGY, VOLCANOLOGY
and applied topics on Environment, Archaeometry and Cultural Heritage*

Applied mineralogical characterization of ilmenite from Kahnuj placer deposit, Southern Iran

Akbar Mehdilo, Mehdi Irannajad* and Bahram Rezaei

Department of Mining & Metallurgical Eng., Amirkabir University of Technology, Tehran, Iran

* Corresponding author: irannajad@aut.ac.ir

Abstract

Kahnuj placer deposit contains ilmenite and magnetite as the main valuable minerals. Microscopic and microprobe analyses show that ilmenite occurs in two forms as individual grains and exsolved lamellae within magnetite. Exsolved lamellae of hematite, sphene of different shape and rare rutile and zircon are found as inclusions in ilmenite. According to microprobe analysis data the TiO₂ content of ilmenite (52.1 wt%) with small amounts of Mg and Mn and is very close to the theoretical one (52.6 wt%). Based on the XRF analysis, the maximum content of TiO₂ in the purified ilmenite concentrate without any gangue minerals is obtained at 44 wt%. The low grade of TiO₂ in the purified ilmenite is attributed to the presence of sphene and hematite inside ilmenite. The presence of sphene as a source of Ca and Si can negatively affect the quality of ilmenite concentrate and the further product - titanium dioxide manufactured via chloride and sulphate routes. It is found that the magnetite from the deposit contains about 1.5 wt% of V₂O₃ and can be considered as important source for extraction of vanadium as a by-product.

Key Words: Titanium; placer deposit; ilmenite; magnetite; mineralogy.

Introduction

A survey on the use of titanium in its various forms shows that almost 95% of the titanium is used for the production of white TiO₂ pigment which has extensive application in paint, plastic and paper industries (Nayl et al., 2009 a,b).

Relatively minor quantities are used to produce the metal and titanium chemicals (Lasheen, 2004). Natural rutile, owing to its high titanium content and low levels of impurities, has traditionally been preferred as feed stock for the production of titanium dioxide pigment. Natural rutile is becoming scarcer and consequently

more costly and the alternative method that uses ilmenite is being favored (Samala et al., 2009).

Ilmenite is usually mined from both hard rocks and placer deposits. Currently, placer deposits supply more than half the titanium minerals mined worldwide. These deposits supply variably altered ilmenite and rutile. (Force, 1991). The placer deposits are considered economically viable deposits because of their profitability and easy mineability. In comparison with rutile, ilmenite concentrates have lower titanium content (less than 52.6% TiO₂), but have a significant amount of Fe which poses problems for pigment production. Nevertheless, ilmenite has been used as an alternate feed material for the production of pigment through chemical routes including sulphate and chloride processes. In the sulphate process, ilmenite concentrate and Ti slag are leached with sulphuric acid while TiO₂ pigment is produced from rutile, high purity Ti slag and some TiO₂-rich sand ilmenites via the chloride process (Millet et al., 1994; Chernet, 1999a; Korneliussen, 2000; Samala et al., 2009).

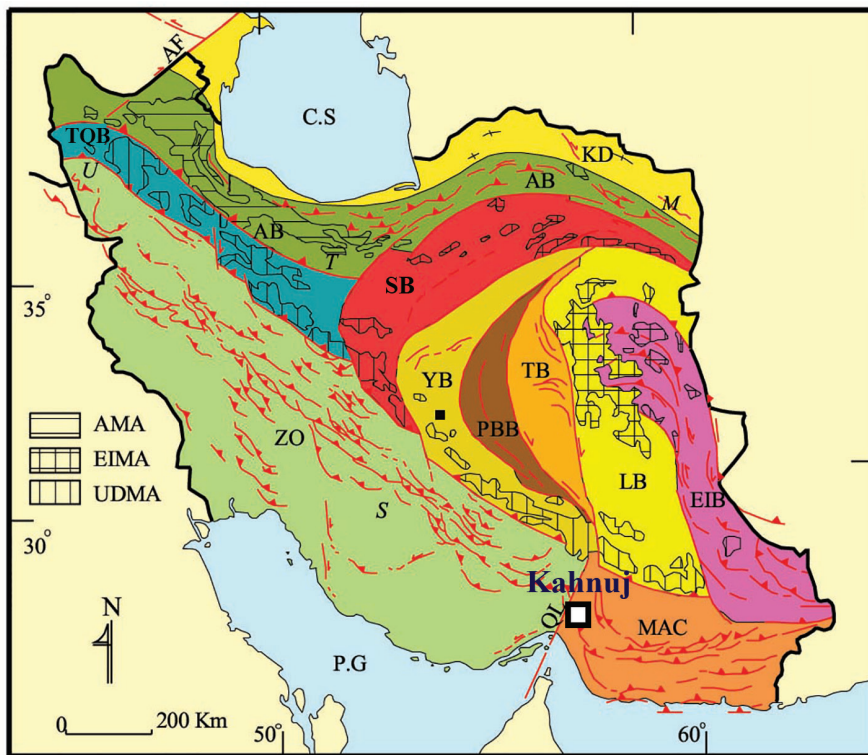
The important factors which affect the reactions of pigment production via sulphate and chloride processes are mineral and chemical composition of the feed and its textural features. Ilmenite is known to contain Cr, V, Mn, Mg, Nb and Ta as minor elements. Such elements as Cr, V and Nb affect the pigment color and their presence may reduce the value of concentrate as pigment plant feed. In general, there is a tendency for ilmenite and Ti slag with low Mg and Cr to be increasingly more attractive relative to raw materials containing high Mg and/or Cr. In TiO₂-pigment production, ilmenite used in the chloride process must have less than 1.5 wt% of MgO. Chromium is a waste problem for the sulphate process and pigment producers. Mg affects the precipitation process and Ca and P cause problems in the crystallization process (Chernet, 1999a and b; Charlier et al., 2007). Also the impurities such as Mg and Ca affect the

stability of the fluidized bed: the boiling points of MgCl₂ and CaCl₂ (the reaction products of Mg and Ca during chlorination) are above the chlorination temperature and so these chlorides accumulate in the fluidized bed (Pistorius, 2008). Partly due to the need to produce good quality pigment, but also due to environmental pressure regarding waste disposal, pigment producers are forced to use feedstock with low level of trace elements (Chernet, 1999a). The ilmenite concentrates that contain significant levels of impurities have a lower market value and therefore there is a considerable incentive for producers to carefully characterize the nature and mode of occurrence of the impurities (Pownceby et al., 2008).

The applied mineralogy is essential for the mineability of titanium deposits as well as for the processes of physical beneficiation of raw materials and chemical routes for production of TiO₂-pigments. In this research, the mineralogical characterization of Kahnuj titanium placer deposit is carried out especially from the applied mineralogical point of view. Kahnuj placer deposit and Qareagahj hard rock deposit are the most important titanium ore reserves in Iran (Irannajad, 1990; Mehdilo and Irannajad, 2010; Mehdilo & Irannajad, 2013). Presently, the mining and production of ilmenite concentrate in Iran takes place only in Kahnuj area, and a concentrate containing 37.5% TiO₂ is produced on a pilot scale.

Kahnuj area

Kahnuj titanium deposit (Figure 1) is located 25 km from Kahnuj city, 170 km from Bandar Abbas and 340 km from Kerman (Rajabzadeh et al., 2011; Irannajad, 1990). The deposit has ophiolitic origin. The Kahnuj ophiolite complex is incomplete being composed mainly of layered gabbros, isotropic gabbros, sheeted dykes, plagiogranites as well as pillow lavas associated with radiolarites and pelagic limestones



A.B.- Alborz belt, A.F.- Aras fault, AMA- Alborz magmatic assemblage, C.S.- Caspian sea, E.I.B.- East Iran belt, EIMA- East Iran magmatic assemblage, K.D.- Kopeh Dagh, L.B.- Lut block, M- Mashhad, M.A.C- Makran accretionary prism, O.L.- Oman line, P.B.B.- Posht-badam block, P.G.- Persian Gulf, S- Shiraz, S.B.- Sabzevar block, T- Tehran, T.B.- Tabas block, T.Q.B.- Tabriz-Qom belt, U- Uromieh, UDMA- Uromieh-Dokhtar magmatic assemblage, Y.B.- Yazd block, Z.O.- Zagros orogen.

Figure 1. Geological map of Iranian ophiolites and location of Kahnuj deposit (Rajabzadeh et al., 2011).

(Rajabzadeh et al., 2011). This area is considered as a junction of Iran's three main structural zones, and is restricted by Lout block in the north, Sanandaj-Sirjan zone in the west and northwest, Jazmourian in the east and Makran zone in the south (Ghazi et al., 2004). The Kahnuj ophiolitic complex is emplaced as a horst structure between two major north-south trending fault zones of Jiroft and Sabzevaran (Rajabzadeh et al., 2011). The general prolongation of Kahnuj

ophiolite and Jiroft and Sabzvaran faults is north-south (N-S). The Ganj, Dare Anar, Chah Mirak and Bidak volcanic-alluvial units of Upper Cretaceous are located in the margin of ophiolite (Ghazi et al., 2004). The gabbroic units of Kahnuj ophiolite are divided into upper and lower gabbros. The upper gabbros are located in the western part of the ophiolite while the lower gabbros form its eastern and higher parts (Rajabzadeh et al., 2011). Some researchers

have determined the geological age of the Kahnuj ophiolite from Cretaceous to Paleocene (Rajabzadeh et al., 2011). The other researchers assume that the Kahnuj ophiolite containing three separate magmatic series have ages from Upper Precambrian - Lower Paleozoic to Upper Paleocene-Eocene (Rajabzadeh et al., 2011; Kananian et al., 2001).

Materials and methods

Series of samples were collected from 25 exploration shafts (with 3-9 m depth) excavated in the studied area. For laboratory experiments the samples were treated according to the scheme shown in Figure 2.

The chemical composition of the prepared materials was determined using X-ray fluorescence analysis (XRFA, Philips X Unique

II). Their phase composition was determined with XPERT MPD diffractometer employing $CuK\alpha$ radiation. The polished and thin sections were used for characterizing the ore and rock-forming minerals and their textural relationships by reflected and transmitted light microscopy. The scanning electron microscopy (SEM) studies were performed using Philips XL30 equipped with DX4 EDX analyzer. The electron microprobe analysis (EMPA) was carried out on a Cameca SX 100 equipped with five wavelength dispersive spectrometers (WDX) at 15 kV acceleration voltage and 100 s counting time both in point and area (about $25 \mu m^2$) regimes. For SEM and EMPA the polished sections were preliminary coated with carbon. The calculation of FeO and Fe_2O_3 from FeO_t (total FeO) obtained by electron microprobe analysis, was performed using GabbroSoft 2012.

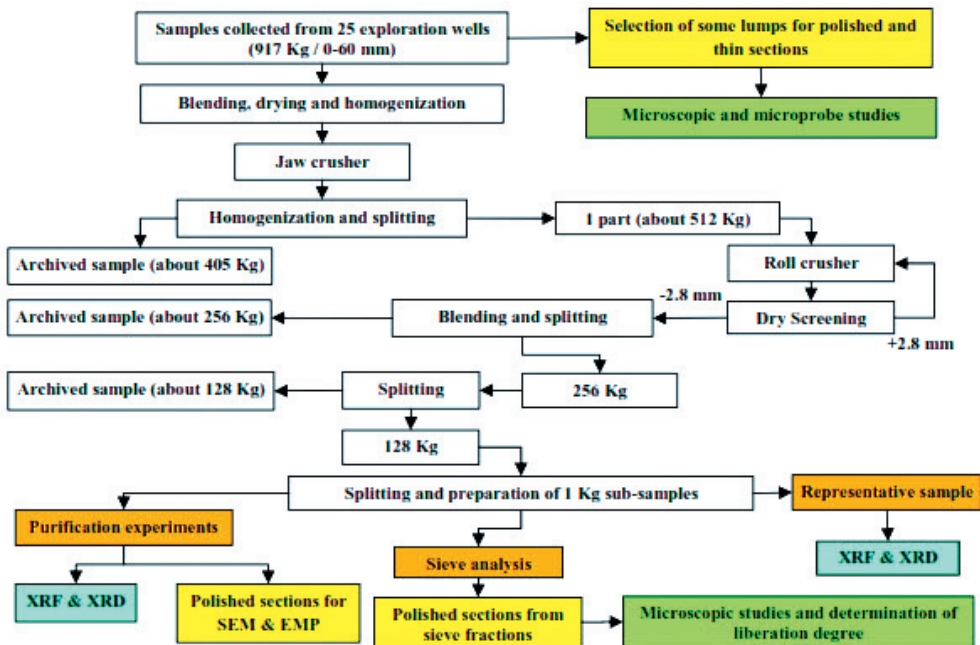


Figure 2. Schematic procedure of sample preparation and characterization.

Results and discussion

Chemical composition

The chemical analysis of a representative (averaged) sample obtained according to the scheme in Figure 2 is shown in Table 1. The content of TiO_2 is 3.65% which is close to some beach sands deposits. Sulphur and phosphorus contents in Kahnij deposit are very low. The X-Ray diffraction (XRD) pattern presented in Figure 3 shows that ilmenite and magnetite are the main valuable minerals in the studied ore. The most important gangue minerals present in the studied samples are plagioclase, pyroxene and amphibole. Albite as Na dominated phase is the most important plagioclase while diopside

and augite are dominant pyroxene minerals. Some diffraction peaks of quartz were also observed in the X-Ray diffraction pattern.

Light microscopy studies

The study of polished sections by reflected light microscopy confirms the XRD and XRFA data that ilmenite and magnetite are the main opaque and valuable minerals in the ore (Figure 4 a,b). The size of ilmenite grains varies in wide range from 50 to 500 μm . The peripheral parts of some ilmenite grains are characterized by cataclastic texture with fractures filled by gangue minerals. The ilmenite grains are often angular and interlocked with gangue minerals.

Table 1. Chemical composition (wt %) of the representative sample.

TiO_2	Fe_2O_3	SiO_2	Al_2O_3	CaO	MgO	Na_2O	K_2O	P_2O_5	MnO	SO_3	L.O.I	Total
3.65	15.15	45.3	13.65	9.57	5.5	2.93	0.31	0.27	0.17	0.33	2.96	99.79

* The total iron is presented as Fe_2O_3 .

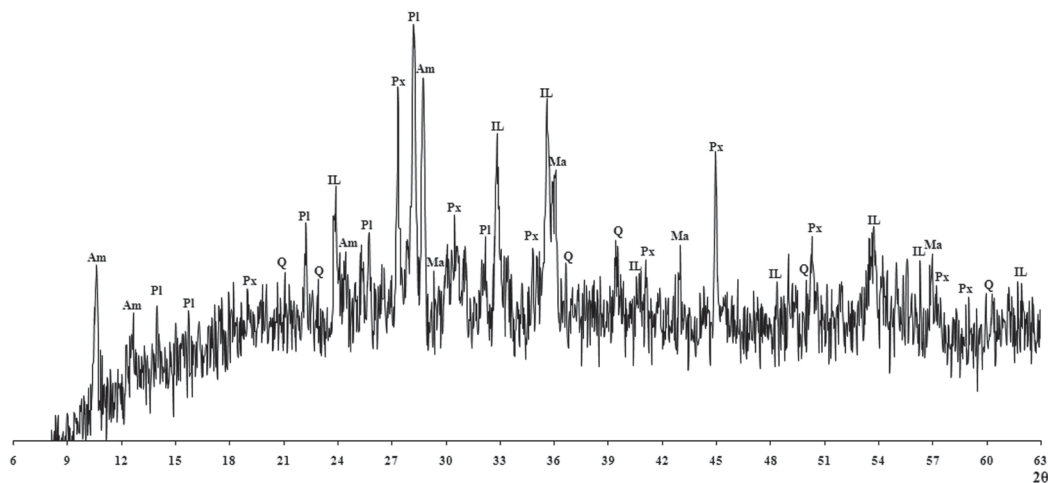


Figure 3. XRD pattern of the representative sample (IL - ilmenite, Ma - magnetite, Pl - plagioclase, Px - pyroxene, Am - amphibole, Q - quartz).

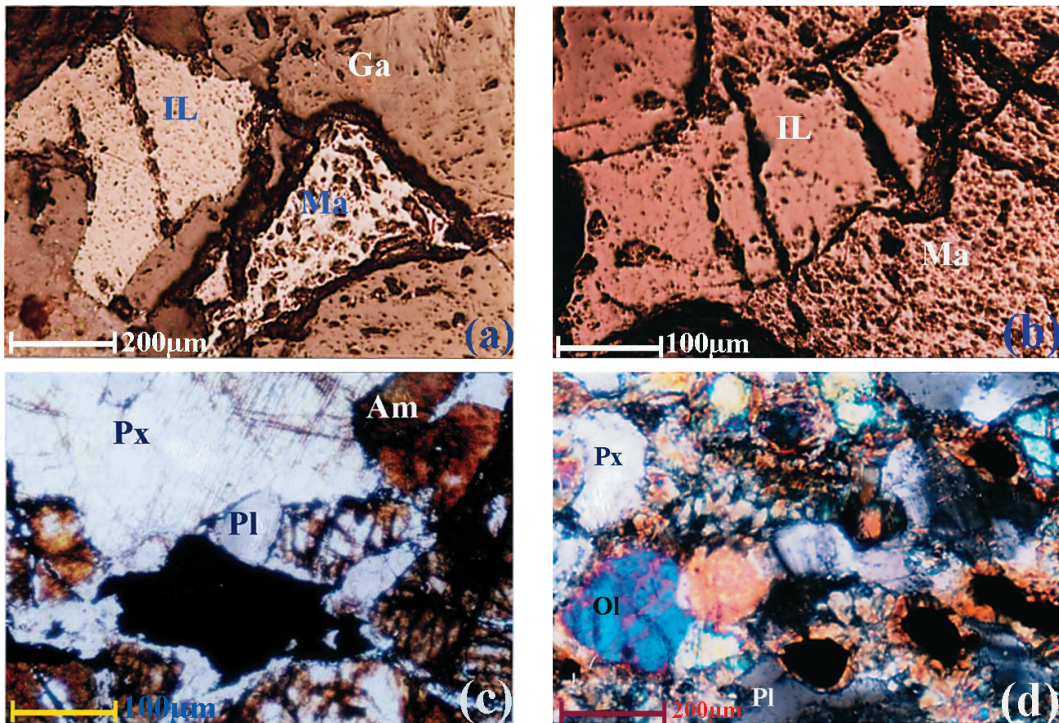


Figure 4. Study by reflected (a and b) and transmitted (c and d) light microscopy. (a) and (b) interlocking between ilmenite and magnetite; the interstices between the ore minerals are filled by gangue minerals; (c) pyroxene and plagioclase with a small amount of amphibole; (d) fine grain of calcic plagioclase and pyroxene with small amount of olivine and amphibole. (IL: Ilmenite, Ma: Magnetite, Px: Pyroxene, Pl: Plagioclase, Am: Amphibole, Ol: Olivine, Ga: Gangue minerals).

Intergrowths of ilmenite and magnetite are also observed. The study of thin sections by transmitted light microscopy shows that plagioclase, pyroxene and amphibole are the main rock forming minerals. Small amounts of quartz, epidote, biotite and olivine are also found in some sections. Figure 4c shows pyroxene and plagioclase with a small amount of amphibole in gabbro-anorthosite which contains relatively a lower amount of opaque minerals (magnetite and ilmenite). Fine grains of plagioclase, pyroxene, olivine and amphibole from fine grained gabbro are shown in Figure 4d. The rock is found to contain more ilmenite and magnetite than gabbro-anorthosite.

SEM and microprobe analyses

The results of SEM and EMPA are given in Figures 5 to 7 and Table 2. Individual grains and exsolved lamellae within magnetite are two observed forms of ilmenite in the ore. The magnetite grains containing exsolution textures of ilmenite lamellae can be referred to ilmenomagnetite (Figure 5a). The analysis of both ilmenites shows that TiO_2 content varies from 49.89 to 55.64 wt%. The average content of TiO_2 is 52.02 wt% which is close to the theoretical content of TiO_2 in ilmenite (52.6 wt%). The average content of FeO is 43.51 wt% (with variation 41.91-45.18 wt%)

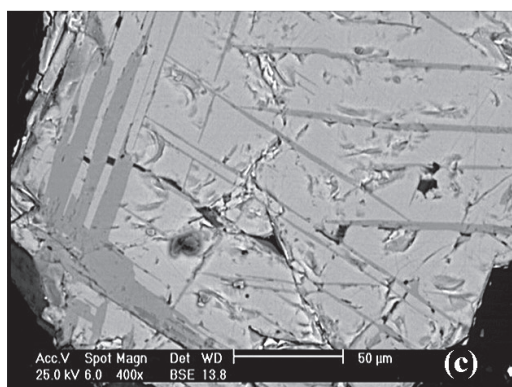
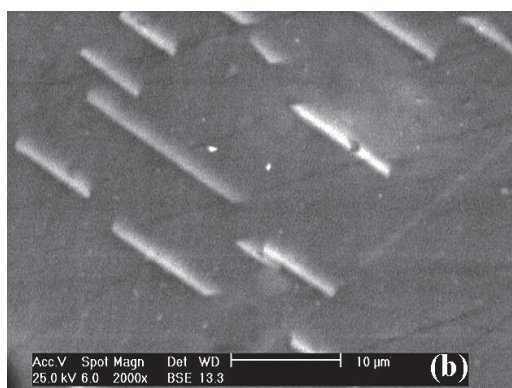
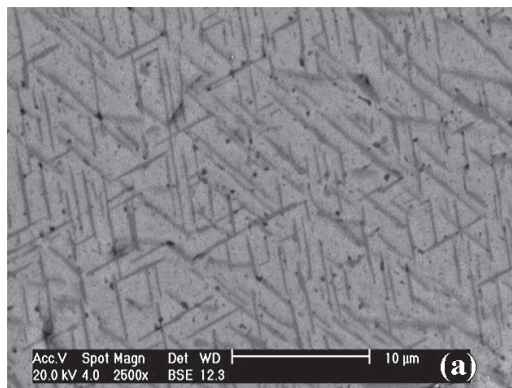


Figure 5. a) Exsolution lamellae of ilmenite within magnetite grain. b) Exsolution lamellae of hematite within ilmenite. c) Exsolution lamellae of ilmenite within titanomagnetite.

which is about 4 wt% lower than its theoretical content in FeTiO_3 (47.4 wt%). This is due to the replacement of some Fe^{2+} ions in the ilmenite lattice by Mg and Mn; which their content as MgO and MnO varies from 0.38 to 2 wt% and 0.83 to 2.23 wt%, respectively. The average contents of FeO and Fe_2O_3 were calculated 42.26% and 1.37%, respectively. Therefore the content of hematite component in the composition of ilmenite is estimated 1-2%. The contents of other impurities such as CaO, P_2O_5 , SiO_2 and Al_2O_3 are negligible. The average contents of V and Cr as TiO_2 pigment coloring metals in the ilmenite structure are 0.26% V_2O_3 and 0.073% Cr_2O_3 . From microprobe analysis, it is concluded that the most important substituent elements in the studied ilmenite are Mg, Mn and V. Mg^{2+} and Mn^{2+} mainly substitute for Fe^{2+} and V^{3+} or V^{4+} substitutes for Ti^{4+} .

BSE images of some ilmenite grains (Figure 5b) allow to reveal the presence of light exsolution lamellae with thickness up to 1 micron. As evidenced by microprobe analysis (Table 2), these lamellae containing more Fe_2O_3 and less TiO_2 can be called hematite or hemoilmenite. Approximately 60% of these lamellae are formed by hematite component. Unlike these lamellae, there are some other lamellae with higher content of TiO_2 (up to 46 wt%). These lamellae containing more than 50 % FeO can be known as high Fe content ilmenite. Based on the calculation of the average contents of FeO and Fe_2O_3 , the hematite component in these lamellae is approximated 13-14%. The impurities such as Mg, Mn, V and Cr substitute for Fe in these lamellae. The contents of V and Cr in hematite or hemoilmenite and also in high Fe content ilmenite phases are higher than that in the ilmenite matrix.

In addition to granular ilmenite, ilmenite exsolution lamellae of the trellis and sandwich types are concentrated in the cores of magnetite crystals. Trellis intergrowths involve thin ilmenite lamellae parallel to all $\{111\}$ planes of

Table 2. Microprobe analyses of ilmenite, magnetite, titanomagnetite and Exsolution phases in wt%.

Phase		TiO ₂	FeO _T *	MnO	V ₂ O ₅	P ₂ O ₅	CaO	MgO	SiO ₂	Al ₂ O ₃	Cr ₂ O ₃	Total	FeO	Fe ₂ O ₃
ilmenite	1	50.29	45.18	2.23	0.57	0.00	0.00	1.44	0.02	0.02	0.03	99.98	40.45	5.26
	2	49.89	45.08	0.83	0.40	0.00	0.02	1.7	0.06	0.02	0.04	98.04	41.06	4.47
	3	50.84	43.82	1.13	0.00	0.00	0.01	1.76	0.06	0.06	0.01	97.69	41.52	2.56
	4	50.69	43.5	1.26	0.19	0.04	0.03	0.83	0.08	0.1	0.50	97.29	42.91	0.66
	5	55.64	42.06	0.90	0.39	0.01	0.06	1.51	0.04	0.03	0.09	100.76	42.06	0.00
	6	51.75	43.43	1.46	0.11	0.02	0.03	0.38	0.06	0.01	0.02	97.46	43.43	0.00
	7	50.50	44.34	0.98	0.39	0.01	0.01	0.53	0.03	0.06	0.00	96.85	43.52	0.91
	8	51.37	43.92	1.26	0.29	0.01	0.02	1.16	0.05	0.04	0.10	98.30	42.91	1.12
	9	52.00	43.53	1.31	0.16	0.02	0.03	1.82	0.04	0.06	0.04	99.01	42.22	1.45
	10	54.22	41.83	1.22	0.21	0.00	0.00	2.00	0.00	0.03	0.00	99.57	41.83	0.00
	11	53.60	42.84	1.16	0.26	0.00	0.02	1.68	0.08	0.00	0.00	99.75	42.84	0.00
	12	53.59	42.41	1.47	0.19	0.01	0.01	1.93	0.00	0.08	0.07	99.79	42.41	0.00
	Average		52.02	43.51	1.27	0.26	0.01	0.02	1.40	0.043	0.043	0.075	98.71	42.26
SD		1.808	1.061	0.363	0.155	0.012	0.017	0.548	0.027	0.030	0.138	1.265	0.936	1.817
Sphene	1	38.76	17.67	0.66	0.04	0.02	17.44	0.03	21.63	3.21	0.03	99.52	-	-
	2	41.66	29.16	0.81	0.32	0.05	10.30	0.23	14.33	1.73	0.13	98.74	-	-
	3	38.10	0.89	0.16	0.40	0.00	28.15	0.00	30.27	0.98	0.00	99.17	-	-
	Average	39.51	15.91	0.54	0.25	0.02	18.63	0.09	22.08	1.97	0.05	99.14	-	-
SD	1.894	14.217	0.340	0.189	0.025	8.984	0.125	7.979	1.135	0.068	0.391	-	-	
Hematite lamellae	1	3.43	85.44	1.31	0.81	0.04	0.04	0.24	0.13	0.10	0.15	91.69	31.95	59.44
	2	3.25	84.93	1.19	0.77	0.00	0.07	0.41	0.09	0.07	0.21	92.00	31.35	59.55
	3	3.52	85.21	1.24	0.64	0.0	0.07	0.58	0.12	0.05	0.19	91.62	31.52	59.67
	4	1.09	87.9	1.36	0.79	0.01	0.05	0.49	0.10	0.04	0.28	92.11	29.58	64.81
	Average	2.82	85.87	1.27	0.75	0.01	0.06	0.43	0.11	0.06	0.21	91.60	31.10	60.87
SD	1.16	1.37	0.075	0.077	0.019	0.015	0.144	0.018	0.026	0.054	0.237	1.044	2.630	
ilmenite lamellae with high Fe content	1	46.02	50.11	0.95	0.44	0.0	0.05	1.33	0.11	0.06	0.12	99.19	38.14	13.30
	2	44.96	51.28	1.03	0.60	0.03	0.03	1.33	0.08	0.04	0.16	99.56	37.10	15.76
	3	45.82	50.47	0.89	0.48	0.02	0.00	1.18	0.12	0.00	0.12	99.12	38.37	13.45
	4	45.92	50.51	0.84	0.41	0.04	0.04	1.14	0.09	0.1	0.09	99.18	38.49	13.36
	5	46.96	49.97	0.91	0.51	0.0	0.01	0.40	0.05	0.11	0.13	99.10	40.66	10.34
	Average	45.94	50.47	0.92	0.49	0.02	0.03	1.08	0.09	0.06	0.12	99.23	38.55	13.24
SD	0.71	0.51	0.07	0.07	0.02	0.02	0.39	0.03	0.04	0.03	0.19	1.30	1.92	
Magnetite	1	1.49	86.63	0.12	1.41	0.00	0.01	0.20	0.00	0.37	0.55	90.98	30.96	61.87
	2	1.48	87.31	0.07	1.48	0.00	0.03	0.34	0.02	0.54	0.52	91.98	31.32	62.22
	Average	1.49	86.97	0.10	1.45	0.00	0.02	0.27	0.01	0.46	0.54	91.48	31.14	62.05
	SD	0.01	0.48	0.04	0.05	0.00	0.01	0.10	0.01	0.12	0.02	0.71	0.254	0.247
Ilmenite lamellae	1	53.47	43.71	1.03	0.22	0.00	0.03	0.83	0.02	0.04	0.08	99.43	43.71	0.00
	2	53.72	43.53	1.16	0.18	0.02	0.01	0.72	0.03	0.02	0.10	99.49	43.53	0.00
	Average	53.60	43.62	1.10	0.20	0.01	0.02	0.78	0.03	0.03	0.09	99.46	43.62	0.00
	SD	0.18	0.13	0.09	0.03	0.01	0.01	0.08	0.01	0.01	0.01	0.04	0.13	0.00
Titanoma-gnetite	1	6.10	84.60	0.24	1.18	0.00	0.08	0.43	0.16	0.47	0.48	93.74	35.78	54.26
	2	7.63	82.33	0.19	1.09	0.02	0.11	0.51	0.12	0.50	0.41	92.91	36.67	50.74
	3	7.80	81.84	0.24	0.98	0.04	0.09	0.48	0.15	0.39	0.45	92.46	36.70	50.16
	Average	7.18	82.92	0.22	1.08	0.02	0.09	0.47	0.14	0.45	0.45	93.04	36.38	51.72
	SD	0.94	1.47	0.03	0.10	0.02	0.02	0.04	0.02	0.06	0.04	0.65	0.522	2.219

SD: Standard deviation.

* The total iron is presented as FeO_T.

the host magnetite and sandwich intergrowths are thick ilmenite lamellae generally restricted to one of the {111} planes of magnetite (Mucke, 2003). As seen from Table 2, the chemical composition of these lamellae is nearly close to that of the ilmenite grains. The average content of TiO_2 in the magnetite grains is almost 1.5 wt% but the TiO_2 content of some magnetite grains varies in the range of 2-10 wt%. The magnetite phases containing higher amount of Ti can be known as titanomagnetite (Figure 5c).

The important isomorphous impurity elements in magnetite and titanomagnetite are V, Cr and Al. Their average contents presented in oxide form (in wt%) in magnetite and titanomagnetite are: V_2O_3 - 1.45 and 1.08, Cr_2O_3 - 0.46 and 0.45, Al_2O_3 - 0.54 and 0.45, respectively. Thus, magnetite and titanomagnetite can be a valuable source for vanadium extraction.

Figures 6a and 6b show replacement of ilmenite (light-grey) by sphene (dark-grey). Microprobe analysis (Table 2), X-ray maps of Ti (6c), Fe (6d), Ca (6e), and Si (6f) and X-ray diffraction analysis reveal that the dark-gray parts are sphene (CaTiSiO_5). Sphene is observed as elongated and angular shapes within ilmenite (Figures 6 and 7). The thickness of elongated parts and also the sizes of other shape sphenes are lower than 20 microns. As seen from Table 2, the most important impurities in the sphene structure are Al and Fe substituting for Ti (Frost et al., 2001). The average contents of FeO and Al_2O_3 in the sphene phase are 15.91 and 1.97 wt%, respectively. In the Kahunj deposit, the sphene mineral probably occurs via reaction of ilmenite with quartz and plagioclase minerals.

Rutile is another titanium containing mineral which is found in intergrowth with ilmenite, magnetite and sphene (Figure 7). Rutile and sphene occur as discrete crystals adjacent to each other or granular intergrowths. The SEM and microprobe analysis revealed the presence of insignificant amount of zircon (smaller than 10 μm) within ilmenite.

Liberation degree

After sieve analysis (Figure 2), several polished sections were prepared from each of seven size fractions (in μm): 2800+2000 μm , -2000+850 μm , -850+500 μm , -500+300 μm , -300+150 μm , -150+75 μm and -75 μm , and further studied in scanning electron microscope. Series of BSE images taken from different places of each polished section were used for counting the liberated and locked ilmenite grains. Then the percent of liberation degree is calculated using equation 3 for all size fractions. The results as percent of liberation degree versus size fraction are shown in Figure 8. Based on these results, the liberation degree of ilmenite was determined as 200 microns:

$$LD(\%) = \frac{n_L}{n_L + n_I} \times 100 \quad (1)$$

where n_L is the total number of liberated ilmenite in all images of each polished section and n_I is the number of interlocked ilmenite in all images of each polished section.

Purification of ilmenite

One of the sub-samples prepared according to the scheme shown in Figure 2 was ground under 200 μm , and purified applying several stages of tabling, low and high intensity magnetic separation methods. The obtained concentrates were washed several times with distilled water and dried at room temperature. Examination under binocular microscope showed that the ilmenite grains were with clean surfaces and free of gangue minerals.

The chemical composition of purified ilmenite is given in Table 3. The higher content of CaO and SiO_2 is due to the presence of sphene (CaTiSiO_5) evidenced by X-ray diffraction (Figure 9) and is also observed in SEM. The other important impurities in this sample are

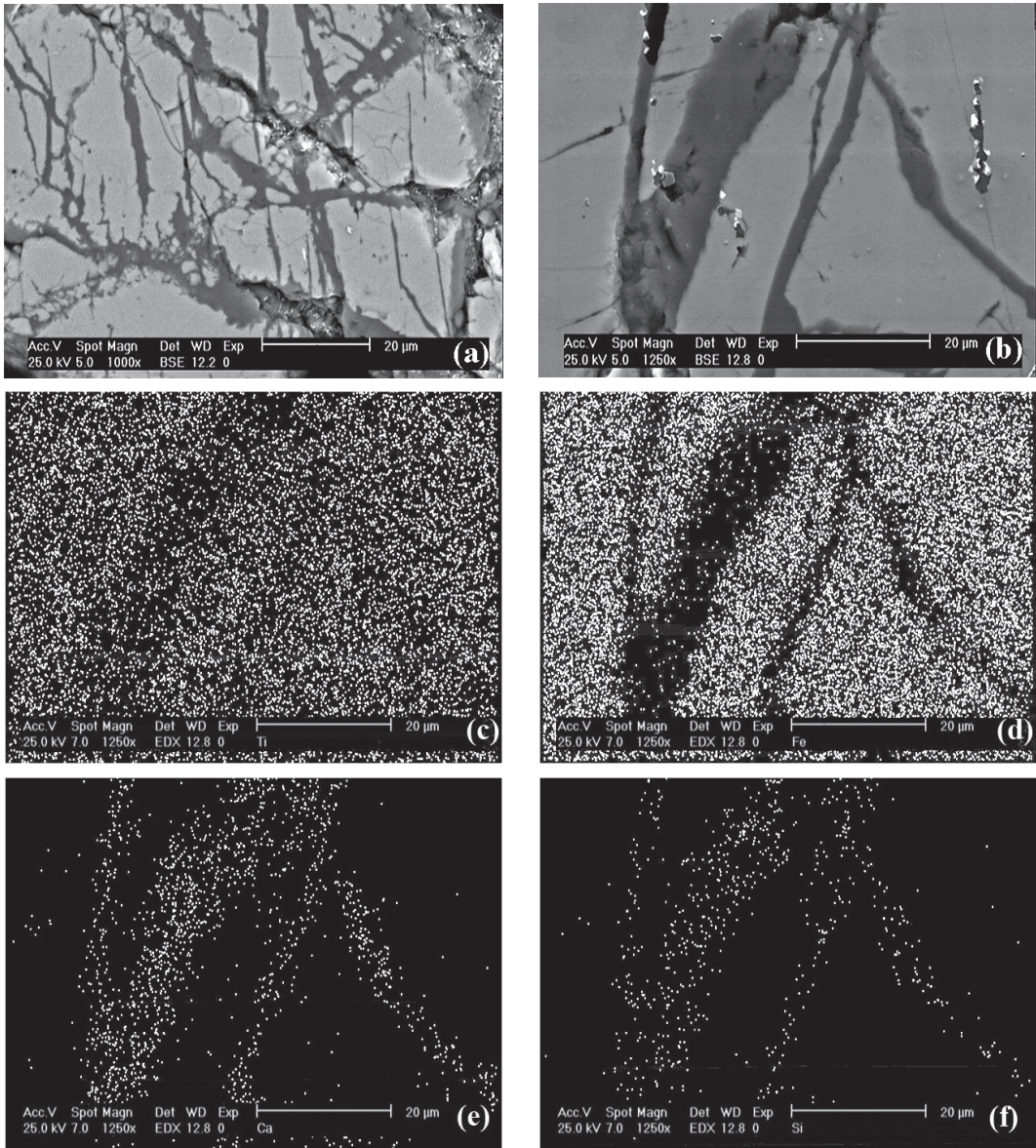


Figure 6. (a) and (b) BSE images and (c-f) X-Ray maps of TiKa (c), FeKa (d), CaKa (e), and SiKa (f) in Figure b.

MgO and MnO which are probably related to the geikielite ($MgTiO_3$) and pyrophanite ($MnTiO_3$) components in the composition of ilmenite. Al_2O_3 content is about 1.2% and most

probably originates from the established sphene. The content of Zr in the purified ilmenite is 440 ppm and most probably is related to the zircon inclusions in ilmenite.

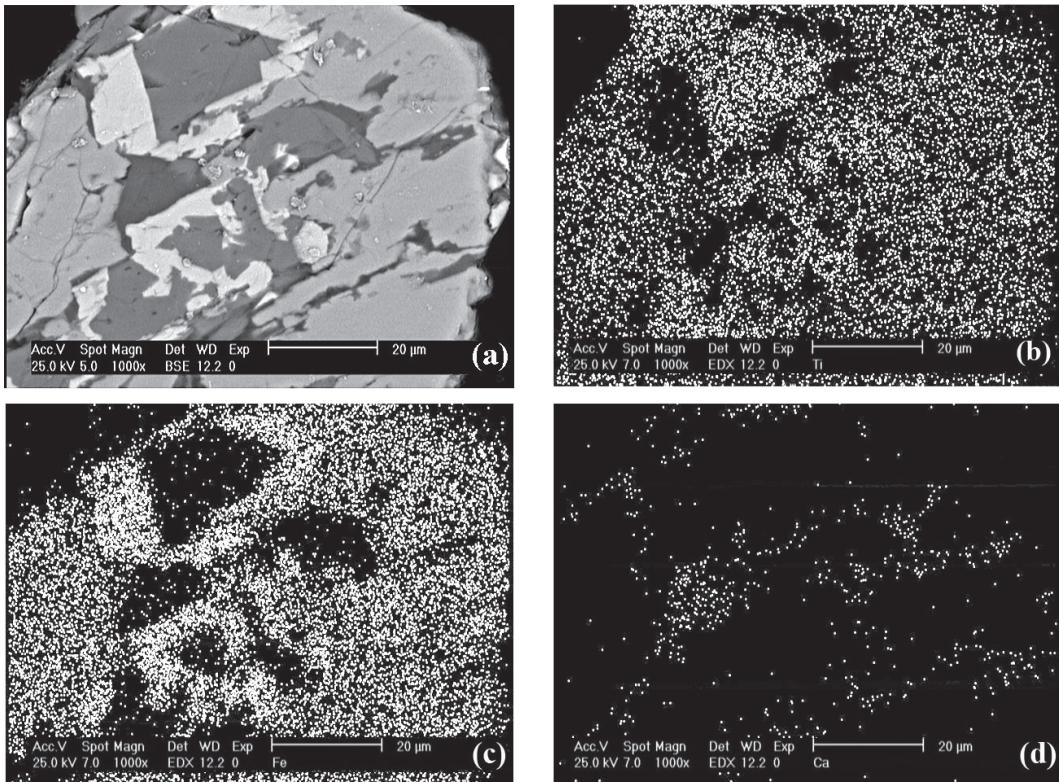


Figure 7. (a) BSE image and (b-d) X-Ray maps of TiKa (b), FeKa (c), and CaKa (d) in Figure a.

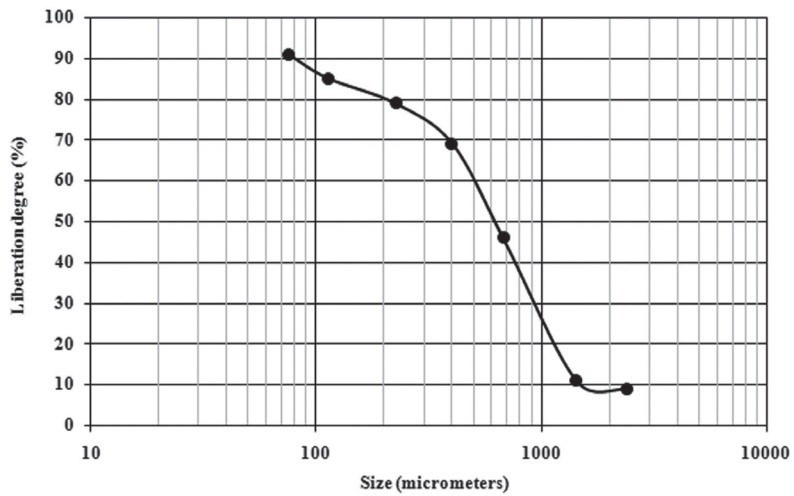


Figure 8. Liberation degree of ilmenite determined by grain counting method.

Table 3. Chemical composition (wt%) of purified ilmenite sample.

TiO ₂	Fe ₂ O ₃	MnO	V ₂ O ₃	P ₂ O ₅	CaO	MgO	SiO ₂	Al ₂ O ₃	Cr ₂ O ₃	Co ₃ O ₄	ZrO ₂	Nb ₂ O ₅	Total
43.9	45.90	1.15	0.31	0.091	1.51	1.84	3.7	1.19	0.04	0.022	0.044	0.012	99.71

* The total iron is presented as Fe₂O₃.

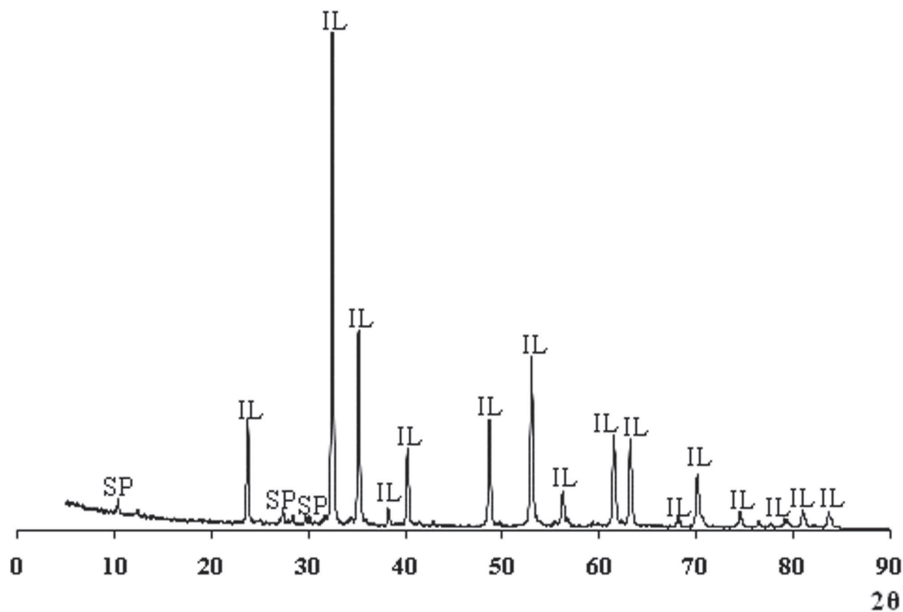


Figure 9. XRD pattern of purified ilmenite (IL = Ilmenite, SP = Sphene).

Conclusion

Ilmenite and magnetite are the main valuable minerals in the Kahanuj placer deposit. The negligible amount of rutile and zircon are found as inclusions mostly in ilmenite grains. In addition of ilmenite grains, some exsolution lamellae of ilmenite were found in magnetite. The lamellar ilmenite due to its small thickness < 5 μm is not recoverable by physical separation methods. However The TiO₂ content of studied ilmenite (52.06%) is very close to its theoretical content in the ilmenite structure (52.6%), but

the structural impurities, hematite exsolutions and sphene inclusions in ilmenite make it impossible to achieve an ilmenite concentrate containing higher than 44 % TiO₂. Mg and Mn as structural impurities result in the formation of geikielite (MgTiO₃) and pyrophanite (MnTiO₃) components in ilmenite. The average content of Fe³⁺ in ilmenite component varies from 1 to 1.5%. Therefore it is concluded that there are solid solutions of ilmenite (FeTiO₃), hematite (Fe₂O₃), geikielite (MgTiO₃) and pyrophanite (MnTiO₃). Elevated contents of SiO₂, Al₂O₃ and CaO in the purified ilmenite correspond to

the sphene inclusions while the higher content of Fe can be attributed to the hematite exsolutions and/or ilmenite-hematite solid solutions. These impurities could negatively affect the pigment production processes via sulphate or chloride routes.

The concentrations of V and Cr as pigment colorizing elements in the Kahnúj ilmenite are closely related to the hematite exsolutions. Their contents in ilmenite concentrate, however, are negligible to have a negative impact on the TiO₂ pigments. These two elements are mainly concentrated in magnetite. The magnetite concentrate containing almost 1.5% V₂O₃ can be used to produce vanadium as a by-product.

Acknowledgments

The authors would like to thank the Amirkabir University of Technology for the financial support of this research.

We are also grateful to the anonymous referees for their helpful comments.

References

- Charlier B., Skar Ø., Korneliussen A., Duchesne J.C. and Auwera J.V. (2007) - Ilmenite composition in the Tellnes Fe-Ti deposit, SW Norway: fractional crystallization, postcumulus evolution and ilmenite-zircon relation. *Contributions to Mineralogy and Petrology*, 154, 119-134.
- Chernet T. (1999a) - Effect of mineralogy and texture in the TiO₂ pigment production process of Tellnes ilmenite concentrate. *Mineralogy and Petrology*, 67, 21-32.
- Chernet T. (1999b) - Applied mineralogical studies on Australian sand ilmenite concentrate with special reference to its behavior in the sulphate process. *Minerals Engineering*, 12(5), 485-495.
- Force E.R. (1991) - Geology of titanium-mineral deposits, Geological Society of America, Spec. Paper 259.
- Ghazi, A.M., Hassanipak, A.A., Mahonery, J.J. and Duncan R.A. (2004) - Geochemical characteristic, ⁴⁰Ar/³⁹Ar age and original tectonic setting of Band-e-Ziarat-Dar Anar ophiolite, Makran accretionary prism, S. E. Iran. *Tectonophysics*, 393, 175-196.
- Irannajad M. (1990) - Pilot plant flowsheet development of the Kahnúj titanium ore deposit, MSc Thesis, Amirkabir University of Technology, Tehran, Iran (in Persian).
- Kanianian A., Juteau T., Bellon H., Darvishzadeh A., Sabzehi M., Whitechurch H. and Ricou L. (2001) - The ophiolite massif of Kahnúj western Makran (Southern Iran): New geological and geochronological data. *Earth and Planetary Science Letters*, 332, 543-552.
- Korneliussen A., McEnroe A.S., Nilsson L.P., Schiellerup H., Gautneb H., Meyer B.G. and Størseth L.R. (2000) - An overview of titanium deposits in Norway. *Norges geologiske undersøkelse Bulletin*, 436, 27-38.
- Lasheen T.A.I. (2004) - Chemical beneficiation of Rosetta ilmenite by direct reduction leaching. *Hydrometallurgy*, 76, 123-129.
- Mehdilo A. and Irannajad M. (2010) - Applied mineralogical studies on Iranian hard rock titanium deposit. *Journal of Minerals & Materials Characterization & Engineering*, 9 (3), 247-262.
- Mehdilo A. and Irannajad M. (2013). Effects of mineralogical and textural characteristics of ilmenite concentrate on synthetic rutile production. *Arabian Journal of Geosciences*, 6, 3865-3876.
- Millet P., Calka A. and Ninham B.W. (1994) - Reduction of ilmenite by surfactant-assisted mechanochemical treatment. *Journal of Materials Science Letters*, 13, 1428-1429.
- Mucke A. (2003) - Magnetite, ilmenite and ulvite in rocks and ore deposits, petrology, microprobe analyses and genetic implication. *Mineralogy and Petrology*, 77, 215-234.
- Nayl A.A., Awward N.S. and Aly H.F. (2009a) - Kinetics of acid leaching of ilmenite decomposed by KOH Part 2. Leaching by H₂SO₄ and C₂H₂O₄. *Journal of Hazardous Materials*, 168, 793-799.
- Nayl A.A., Ismail I.M. and Aly H.F. (2009b) - Ammonium hydroxide decomposition of ilmenite slag. *Hydrometallurgy*, 98, 196-200.
- Pistorius P.C. (2008) - Ilmenite smelting: the basics. *The Journal of the Southern African Institute of Mining and Metallurgy*, 108, 34-43.
- Pownceby M.I., Sparrow G. J. and Fisher-White M.J. (2008) - Mineralogical characterization of Eucla Basin ilmenite concentrates - First results from a new global resource. *Minerals Engineering*, 21, 587-597.
- Rajabzadeh M.A., Ghorbani M. and Saadati M. (2011) - Mineralization study of titanium in

- Kahnuj ophiolitic complex based on petrological, mineralogical and geochemical data, south of Kerman province. *Journal of Petrology*, Isfahan University, 7, 21-38.
- Frost B.R., Chamberlain K.R., & Schumacher J.C. (2001) - Spinel (titanite): phase relations and role as a geochronometer. *Chemical Geology*, 172, 131-148.
- Samala S., Mohapatra B.K., Mukherjee P.S. and Chatterjee S.K. (2009) - Integrated XRD, EPMA and XRF study of ilmenite and titanium slag used in pigment production. *Journal of Alloys and Compounds*, 474, 484-489.

Submitted, November 2013 - Accepted, February 2015